THE COSMIC/FORMOSAT-3 MISSION

Early Results

BY R. A. ANTHES, P. A. BERNHARDT, Y. CHEN, L. CUCURULL, K. F. DYMOND, D. ECTOR, S. B. HEALY, S.-P. HO, D. C. HUNT, Y.-H. KUO, H. LIU, K. MANNING, C. MCCORMICK, T. K. MEEHAN, W. J. RANDEL, C. ROCKEN, W. S. SCHREINER, S. V. SOKOLOVSKIY, S. SYNDERGAARD, D. C. THOMPSON, K. E. TRENBERTH, T.-K. WEE, N. L. YEN, AND Z. ZENG

The COSMIC radio occultation mission represents a revolution in atmospheric sounding from space, with precise, accurate, and all-weather global observations useful for weather, climate, and space weather research and operations.

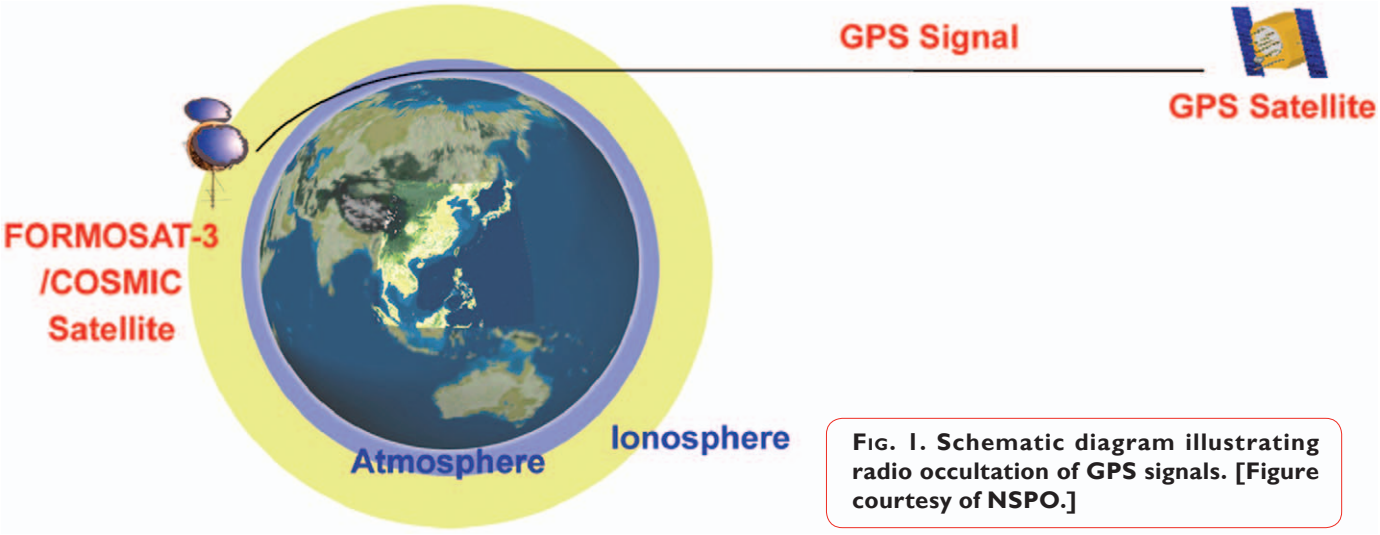

FIG. 1. Schematic diagram illustrating radio occultation of GPS signals. [Figure courtesy of NSPO.]

The global positioning system (GPS) radio-occultation (RO) limb-sounding technique for sounding Earth's atmosphere was demonstrated by the proof-of-concept GPS Meteorology (GPS/MET) experiment in 1995–97 (Ware et al. 1996). Following GPS/MET, additional missions, that is, the Challenging Minisatellite Payload (CHAMP; Wickert et al. 2001) and the Satellite de Aplicaciones Cientificas-C (SAC-C; Hajj et al. 2004), have confirmed the potential of RO sounding of the ionosphere, stratosphere, and troposphere.

At 0140 UTC 15 April 2006, six microsatellites were launched into a circular, 72° inclination orbit at an altitude of 512 km from Vandenberg Air Force Base, California (Cheng et al. 2006). The mission is a collaborative project of the National Space Organization (NSPO) in Taiwan and the University Corporation for Atmospheric Research (UCAR) in the United States. The mission is called the Constellation Observing System for Meteorology, Ionosphere, and Climate (COSMIC) in the United States and the Formosa Satellite Mission 3 (FORMOSAT-3) in Taiwan.[1] All satellites began delivering useful data within days ▶

[1] For simplicity we will refer to the mission as COSMIC in this paper.

after the launch (Anthes 2006). This paper summarizes the mission and the early scientific results, with emphasis on the radio-occultation part of the mission.

The primary payload of each COSMIC satellite is a GPS radio-occultation receiver developed by the National Aeronautics and Space Administration's (NASA's) Jet Propulsion Laboratory (JPL). By measuring the phase delay of radio waves from GPS satellites as they are occulted by the Earth's atmosphere (Fig. 1), accurate and precise vertical profiles of the bending angles of radio wave trajectories are obtained in the ionosphere, stratosphere, and troposphere. From the bending angles, profiles of atmospheric refractivity are obtained. The procedures used to obtain stratospheric and tropospheric bending angle and refractivity profiles from the raw phase and amplitude data for the COSMIC mission are described by Kuo et al. (2004).

The radio-occultation method for obtaining atmospheric soundings is summarized by Kursinski et al. (1997) and in a special issue of *Terrestrial, Atmospheric and Oceanic Sciences* (2000, Vol. 1, hereafter *TAO*). *TAO* also describes the RO method; the application of RO to weather, climate, and ionospheric research; and the COSMIC mission. The refractivity N is a function of temperature (T; K), pressure (p; hPa), water vapor pressure (e; hPa), and electron density (n_e; number of electrons per cubic meter),

$$N = 77.6\frac{p}{T} + 3.73\times10^{5}\frac{e}{T^{2}} - 4.03\times10^{7}\frac{n_e}{f^{2}}. \quad (1)$$

In (1), f is the frequency of the GPS carrier signal (Hz).

The refractivity profiles can be used to derive profiles of electron density in the ionosphere, temperature in the stratosphere, and temperature and water vapor in the troposphere. The RO technique and its history, which starts with the exploration of Mars in the 1960s and was later applied to other planets, are described by Yunck et al. (2000).

The COSMIC satellites also carry two other payloads, which were developed by the Naval Research Laboratory (NRL). The tiny ionospheric photometer (TIP) monitors the intensity of emissions that result from the recombination of oxygen ions with electrons at ionospheric altitudes; the observed intensities can be converted to electron density in the ionosphere. The TIP measurements can monitor the electron density depletions associated with ionospheric bubbles that are frequently associated with radio frequency scintillation. The nadir-pointing coherent electromagnetic radio tomography (CERTO) tri-band beacon (TBB) permits ionospheric observations by measuring the phase differences at two or three frequencies using ground-based receivers. Data from the TBB receivers can be used to retrieve the satellite-to-ground total electron content, to allow for high-resolution tomography of the electron density distribution, and to monitor phase and amplitude scintillations induced in radio waves propagating through the ionosphere. Together with the RO observations, these instruments will contribute observations of electron density of unprecedented horizontal and vertical resolution to the operational and research space weather communities.

While the primary scientific goal of COSMIC is to demonstrate the value of near-real-time (NRT) RO observations in operational numerical weather prediction (NWP), some interesting scientific results from COSMIC that are relevant for climate and other atmospheric studies have already been obtained. This paper summaries some of these results and also serves to inform the scientific community about the availability of COSMIC data for research and operations. The observations may be obtained free of charge upon registration on the Web site of the Taiwan

AFFILIATIONS: Anthes, Ector, Hunt, Kuo, Rocken, Schreiner, Sokolovskiy, Syndergaard, Wee, and Zeng—University Corporation for Atmospheric Research, Boulder, Colorado; Bernhardt and Dymond—Naval Research Laboratory, Washington, D.C.; Chen, Liu, Manning, Randel, and Trenberth—National Center for Atmospheric Research, Boulder, Colorado; Cucurull—University Corporation for Atmospheric Research, Boulder, Colorado, and Joint Center for Satellite Data Assimilation, Washington, D.C.; Ho—University Corporation for Atmospheric Research, and National Center for Atmospheric Research, Boulder, Colorado; Healy—European Centre for Medium-Range Weather Forecasts, Reading, United Kingdom; McCormick—Broad Reach Engineering, Golden, Colorado; Meehan—Jet Propulsion Laboratory, Pasadena, California; Thompson—Utah State University, Logan, Utah; Yen—National Space Organization, Hsin-Chu, Taiwan
CORRESPONDING AUTHOR: Ying-Hwa Kuo, UCAR, P.O. Box 3000, Boulder, CO 80307
E-mail: kuo@ucar.edu

The abstract for this article can be found in this issue, following the table of contents.
DOI:10.1175/BAMS-89-3-313

In final form 17 September 2007

Analysis Center for COSMIC (TACC) in Taiwan (at http://tacc.cwb.gov.tw; also available through the UCAR Web site at www.cosmic.ucar.edu/). The UCAR COSMIC Data Analysis and Archival Center (CDAAC) processes the COSMIC data into neutral atmospheric profiles and ionospheric products. The atmospheric profiles are being distributed in NRT to international weather centers via the Global Telecommunication System (GTS) from CDAAC through the National Oceanic and Atmospheric Administration/National Environmental Satellite, Data, and Information Service (NOAA/NESDIS). Raw data and processed data products can also be downloaded from the CDAAC and TACC Web sites, which include convenient data-mining and visualization tools.

Immediately after launch the six satellites were orbiting very close to each other at the initial altitude of 512 km. During the first 17 months following launch the satellites were gradually dispersed into their final orbits at ~800 km, with a separation angle between neighboring orbital planes of 30° longitude. The current and near-final orbital configuration is giving global coverage of approximately 2,000 soundings per day, distributed nearly uniformly in local solar time. During the first few months, however, the close proximity of the satellites permitted a unique opportunity to obtain independent soundings very close (within tens of kilometers or less) to each other, allowing for new estimates of the precision of the RO sounding technique. During the first year, the clusters of closely collocated (in space and time) COSMIC soundings are supporting case studies of mesoscale atmospheric phenomena, such as gravity waves, fronts, and tropical cyclones.

The next sections describe some of the early results from COSMIC. We first present results using the open-loop tracking technique, which eliminates many of the problems affecting early GPS RO missions, such as GPS/MET and CHAMP, which used phase-locked-loop (PLL) tracking. We then show some results from several studies illustrating the impact of COSMIC observations on regional and global models. Next, we show how COSMIC data are useful for climate research and monitoring. We conclude with some results from the ionospheric applications.

OPEN-LOOP TRACKING AND PROFILING THE ATMOSPHERIC BOUNDARY LAYER.

Open-loop tracking technique. In previous RO missions, such as GPS/MET, CHAMP, and SAC-C (until 2005), the radio signals were recorded in the so-called PLL mode, that is, the phase of the RO signal was modeled (projected ahead) by extrapolating the previously extracted phase. The PLL tracking, routinely applied in GPS and other receivers, is known to be an optimal tracking technique for single-tone signals with sufficient signal-to-noise ratio (SNR). However, this technique often fails in the moist lower troposphere because multipath propagation causes strong phase and amplitude fluctuations. This results in significant errors of the extrapolation-based phase model, the loss of SNR, and ultimately the loss of the lock on the signal. For these reasons, PLL tracking, in many cases, does not allow deep penetration of the retrieved profiles into the moist lower troposphere and, especially, below the top of the atmospheric boundary layer (ABL). In addition to these problems, the PLL tracking, which requires sufficient SNR to lock on the signal, cannot be applied for rising occultations. An alternative open-loop (OL) tracking, that is, raw sampling of the complex signal, was applied to planetary occultations (Lindal et al. 1983). However, without a signal model, the OL tracking required a very high sampling rate substantially exceeding the Nyquist limit (defined by the RO signal frequency bandwidth). The application of raw sampling for routine RO sounding of the Earth's atmosphere from satellites is technically not feasible.

To overcome these problems, a model-based OL tracking technique was developed for use in the moist troposphere for both setting and rising occultations (Sokolovskiy 2001). In OL tracking the receiver model does not use feedback (i.e., the signal recorded at an earlier time), but is based instead on a real-time navigation solution and an atmospheric bending angle model.[2] The model-based OL technique allows tracking of complicated RO signals under low SNR, sampling at a rate close to the Nyquist limit, tracking of both setting and rising occultations, and penetration of the retrieved profiles below the top of the ABL. The OL tracking was implemented and tested for the first time by JPL in the SAC-C RO receiver in 2005, and the RO signals were successfully inverted (Sokolovskiy et al. 2006a). For the first time OL tracking is being routinely applied on COSMIC.

The largest difference between results from OL and PLL tracking is seen in the tropics, where the RO signal structure is most complicated because of the multipath propagation of radio waves. Figure 2 shows a statistical comparison of CHAMP- and COSMIC-retrieved refractivities (between 30°S and 30°N) to

[2] The receiver frequency model is used only for noise filtering and is not used in the postprocessing of the RO signals; thus, it does not directly affect the inversion results.

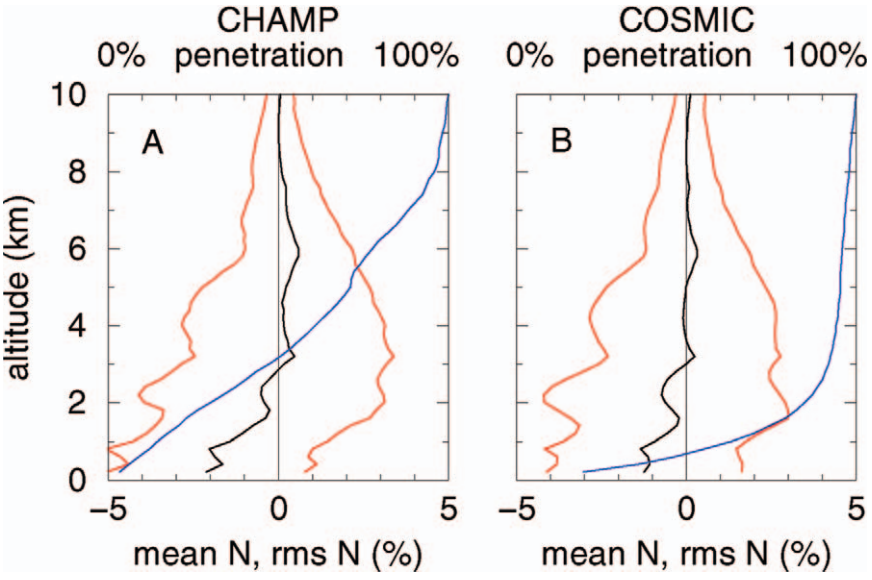

Fig. 2. Statistical comparison of CHAMP and COSMIC RO-retrieved refractivities between 30°S and 30°N to ECMWF global analyses for 28 Aug–22 Sep 2006. The mean deviation (black lines) and ± std dev around the mean (red lines), and the percentage of retrieved profiles that penetrated to a given altitude (blue lines) are shown.

the European Centre for Medium-Range Weather Forecasts (ECMWF) global analysis in the tropics for yeardays 240–265 in 2006. Black and red lines show mean deviation and standard deviation around the mean (both as a fraction of the mean refractivity). Blue lines show penetration, that is, the fraction of the total number of occultation profiles inverted down to a certain altitude. Before the inversion, the CHAMP raw signals were subject to screening for obvious PLL tracking errors (Kuo et al. 2004) and truncation. The truncation basically removes the portions of the retrieved RO profiles with strong refractivity gradients that cause the PLL tracking errors. The conservative nature of the screening results in a trade-off between the depth of penetration and PLL errors. There is no screening of the OL signals, and thus all of the COSMIC RO profiles are equally represented in the statistics. In the process of the inversion, the cutoff altitude for each retrieved profile is determined based on the amplitude of the signal transformed to impact parameter representation by the full spectrum inversion (FSI; Jensen et al. 2003) used by CDAAC. Although discussion of the cutoff algorithm is beyond the scope of this paper, it is important that the same algorithm is applied for both PLL and OL data. It is seen from Fig. 2 that OL tracking results in significantly deeper penetration below 8 km and a reduction of the negative *N* bias in the lower troposphere (below ~2 km). The negative *N* bias in the lower troposphere has been the subject of research for a number of years (Rocken et al. 1997). Possible reasons for the negative *N* bias are i) tracking errors under low SNR (Ao et al. 2003; Beyerle et al. 2006), ii) the presence of superrefraction induced by strong refractivity gradients on top of the ABL (Sokolovskiy 2003; Ao et al. 2003; Xie et al. 2006), iii) an insufficient tracking depth of RO signals (Sokolovskiy 2003), and iv) bias of the ancillary data used for comparison. We believe that reduction of the *N* bias with the use of OL tracking is caused by the reduction of tracking errors and by an increase of the tracking depth.

The remaining negative *N* bias below ~2 km in Fig. 2 may be related to atmospheric propagation effects, such as superrefraction. Biases in the ECMWF analyses, especially water vapor (Simmons et al. 2007), could also contribute to the difference. Further improvement of the accuracy of signal modeling in next-generation RO receivers (and an increase of the antenna gain) will help verify this hypothesis. The negative *N* bias between 2 and 3 km may be related to the inadequate resolution of the sharp top of the ABL by the analysis (as can be seen in Fig. 5, discussed later). Finally, the small positive *N* bias of CHAMP compared to COSMIC between ~2 and 8 km (where CHAMP substantially loses penetration) is consistent with the bias found with the simulations of the PLL tracking (applied in CHAMP receiver) by Beyerle et al. (2006).

The penetration of the RO-retrieved profiles to the Earth's surface depends on a number of factors, such as inversion algorithms, receiver signal-tracking algorithms, terrain, vertical structure of the refractivity profile, receiver antenna gain, and azimuth of the occulted GPS with respect to the receiving antenna boresight. In order to give a quantitative estimate of COSMIC RO penetration over the oceans, where terrain is not a factor, Fig. 3 shows penetration of about 1,000 setting (solid lines) and rising (dashed lines) occultations over the tropics (red lines) and at high latitudes (blue lines). On average, about 70% of occultations penetrate below 1 km in the tropics and about 90% at high latitudes. Although

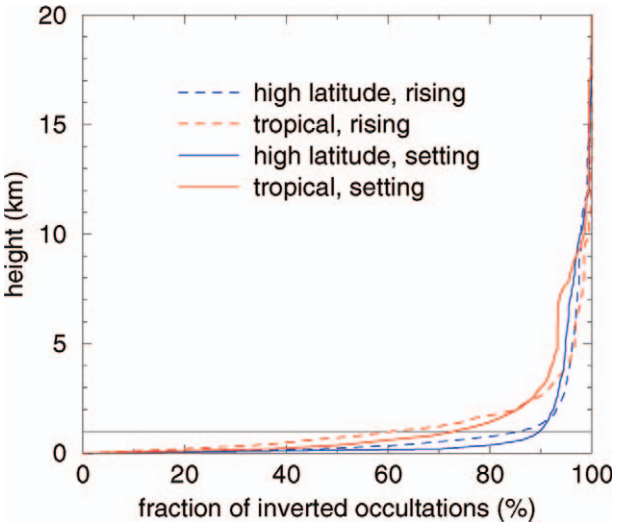

Fig. 3. Penetration of COSMIC rising and setting occultations to mean sea level over the ocean in the tropics and at high latitudes.

theoretically there is no difference between the OL tracking of rising and setting occultations, the slight difference in penetration reflects the difference of the accuracy of the receiver models for rising and setting occultations in the COSMIC receivers. The RO penetration can be improved and the differences between the tropics and high latitudes and between rising and setting occultations can be reduced by improving the accuracy of the receiver model and increasing antenna gain in future missions.

Detecting the atmospheric boundary layer. The ABL is the lowermost atmospheric layer directly affected by Earth's surface. Commonly, the boundary between this turbulently mixed layer and the stably stratified atmosphere above is characterized by a temperature inversion and the decrease of relative and absolute humidity, especially in the moist tropics and subtropics. The top of the ABL is sharper and horizontally more homogeneous in the subtropics, where it is often called a trade wind inversion, than in the tropics and over oceans compared to land. The depth of the ABL is an important parameter for numerical weather prediction and climate models.

Figure 4 shows an example of a radiosonde profile of temperature and partial pressure of water vapor and the corresponding refractivity profile in the case of a sharp top of the ABL (based on Fig. 1 in Sokolovskiy et al. 2006b). It is seen that the top of the ABL corresponds to a strong negative gradient in refractivity. This gradient produces significant multipath propagation, resulting in large tracking errors or the loss of lock in RO receivers operating in PLL mode. Thus, monitoring subtropical and tropical ABL is almost impossible with PLL tracking. With OL tracking, the sharp top of the ABL can be determined from the inverted refractivity profile (Sokolovskiy et al. 2006b).

Figure 5 illustrates two examples of the bending angle and refractivity profiles in the subtropics inverted from COSMIC RO signals down to the ocean surface compared to a 21-level ECMWF pressure analysis archived at the National Center for Atmospheric Research (NCAR). The top of the ABL manifests itself in the profile of the bending angle, which is a "rawer" (lower level) observed product, more distinctly than in refractivity. It is important to note that the use of radio holographic inversion methods, such as the FSI, allows sub-Fresnel vertical resolution of about 60 m (Gorbunov et al. 2004). Such high vertical resolution is not achievable by satellite nadir-viewing instruments. Thus, RO data can contribute significant information about the ABL depth to atmospheric models. It is seen that the coarse model analysis, while tending to reproduce the ABL, is not resolving its top. Routine use of a higher-resolution 91-level ECMWF analysis is currently being tested at CDAAC.

As seen from Fig. 5, the altitude corresponding to the largest bending angle change can be used as an estimate of the ABL depth. However, in some cases this altitude may correspond not to the top of the ABL, but to the top of a cloud layer or other inversion above the ABL. The latter information is also potentially useful for atmospheric models. With the large number of occultations, COSMIC is able to provide global maps of

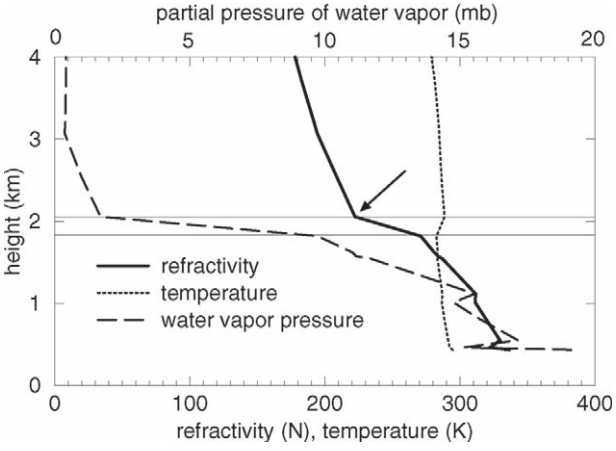

Fig. 4. Temperature, water vapor, and refractivity profiles in the lowest 4 km of the atmosphere, based on a radiosonde (2 Jan 2002; 15.97°S, 5.70°W) showing typical structure of the ABL (Sokolovskiy et al. 2006b).

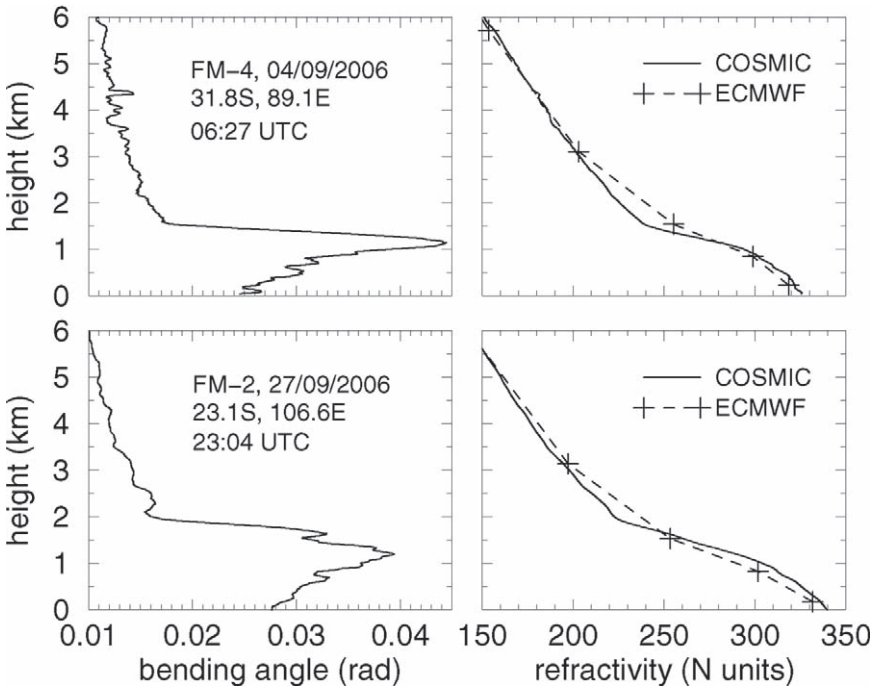

Fig. 5. Examples of COSMIC RO-retrieved bending angle and refractivity profiles in the subtropics, showing the sharp ABL top compared to ECMWF analyses.

are regions of frequent cyclogenesis. This suggests that RO data can be useful for monitoring conditions favoring or accompanying cyclogenesis. COSMIC will allow the study of the global climatology of the ABL, which is not possible with passive nadir-viewing satellite instruments because of insufficient vertical resolution. It is important to note that such studies will comprise not only latitudinal–longitudinal and seasonal ABL variations, but also diurnal variations, because COSMIC provides uniform coverage in local solar time.

PRECISION OF GPS RO MEASUREMENTS.

As noted above, during the first few months after launch, the COSMIC satellites were orbiting in close proximity. This afforded the opportunity to compare soundings from independent instruments and platforms, and thereby obtain estimates of the precision of the RO observations. Figure 7a shows a pair of "dry" temperature profiles retrieved from RO soundings obtained on 3 August 2006 from two satellites that were separated by about 1 km, and a corresponding temperature profile from the National Centers for Environmental Prediction

the ABL and cloud layer depths. An example of such a map is shown in Fig. 6 for 17–30 September 2006. The results are based on occultations that penetrate to at least 0.5 km above sea level and for which the maximum change in bending angle within a 0.3-km-height interval exceeds 0.01 rad. The color of each data point indicates the altitude of the maximum change of bending angles. It is seen that well-defined tops of the ABL by the above criteria occur most often in the subtropics and, especially, more in southern rather than in northern latitudes (this is to be expected for September). Lower heights of the ABL occur toward the western coasts of South America and Africa. The intertropical convergence zone (ITCZ) has significantly fewer occultations that show a well-defined top of the ABL; this is related to general upward motion and convection in the ITCZ. It is interesting to note that some areas, where there are few sharp vertical gradients (e.g., the western equatorial Pacific),

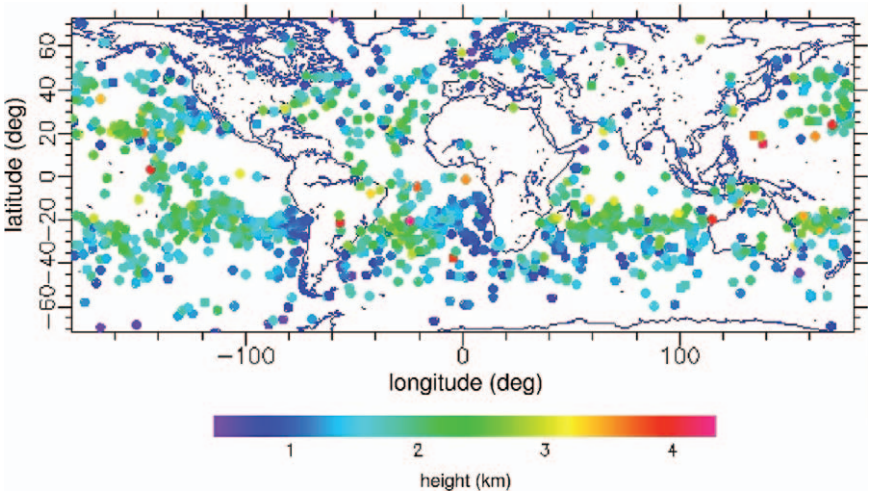

Fig. 6. Map of COSMIC profiles for 17–30 Sep 2006 that reveal sharp tops of the ABL or cloud top. Color code shows the height (km) of the ABL.

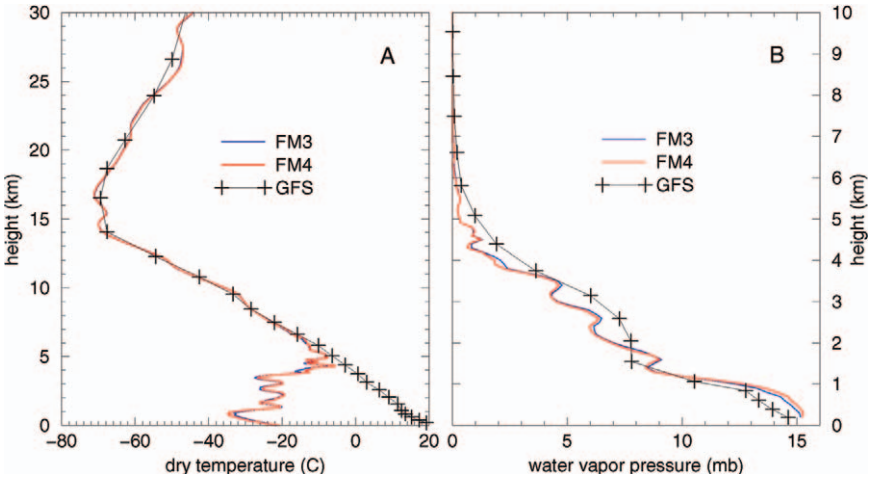

Fig. 7. (a) Vertical profiles of "dry" temperature (blue and red lines) from two independent receivers on separate COSMIC satellites (*FM-3* and *FM-4*) on 3 Aug 2006. The satellites were approximately 5 s apart, which corresponds to a distance separation at the ray tangent point of about 1 km. The soundings are at 21.8°S, 32.9°W. The black line (GFS) is the NCEP analysis of temperature interpolated to the time and location of the COSMIC soundings. (b) Same as in (a), but for water vapor pressure profiles computed from the refractivities using a 1D variational data assimilation scheme. The red and blue lines are difficult to distinguish because they coincide so closely.

(NCEP) Global Forecast System (GFS) model. "Dry" temperatures are computed from the observed refractivity under the assumption that water vapor pressure is zero in Eq. (1). The difference between "dry" temperature and actual (kinetic) temperature in a RO retrieval is due to the presence of water vapor. The two independent soundings in Fig. 7a agree closely, even in the lower troposphere where significant small-scale variability exists due to layers of water vapor. The differences between the two collocated soundings and the GFS model are significant at some levels above 14 km, and are likely due to gravity waves that are present in the RO observations but not the GFS model. In the lowest 6 km the differences are largely due to the presence of water vapor.

Figure 7b shows water vapor profiles obtained from the same RO pair that produced the "dry" temperature soundings in Fig. 7a. The water vapor profiles were generated with a one-dimensional variational data assimilation (1DVAR) algorithm using the NCEP GFS model as the first guess. Although less effective than either three- or four-dimensional variational data assimilation methods in optimally combining GPS RO measurements with NWP background and other independent observations, the computationally cheaper 1DVAR assimilates RO-retrieved profiles at the full vertical resolution provided by the RO. Healy and Eyre (2000) and Palmer et al. (2000) provided overviews of the 1DVAR method and some specific issues pertinent to GPS RO. Very good agreement can be seen in the pairs of RO water vapor profiles. Again, this close agreement does not represent the accuracy of RO water vapor retrievals because many errors, including model temperature errors, are common to both profiles, but it does indicate the precision of the technique in terms of water vapor pressure.

Although it is interesting to look at a few pairs of soundings, it is important to look at the statistics of many comparisons. During the first seven months of the COSMIC operation, we collected over 2,500 pairs of RO soundings from *FM-3* and *FM-4* with the tangent points separated by less than 10 km. The average time difference between soundings that occur within 10 km of each other is 18 s. The statistics of the differences in refractivities for the pairs are shown in Fig. 8 as a function of height. The blue line

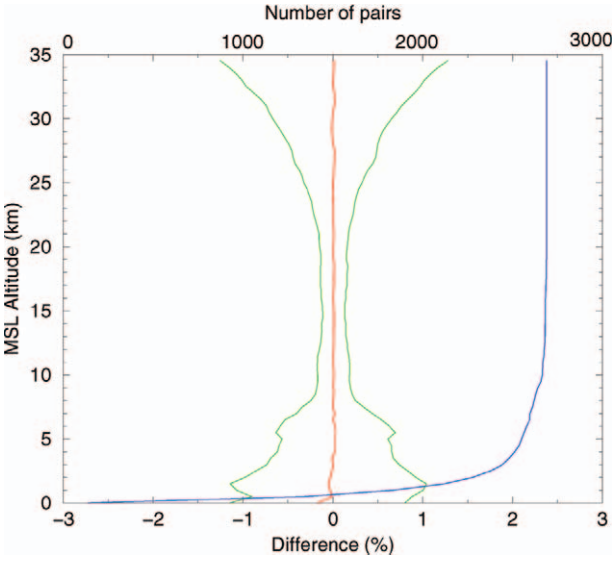

Fig. 8. Difference of pairs of GPS RO measurements (*FM3-FM4*) with tangent point separation less than 10 km. Mean difference shown by red line; standard deviations of the differences shown by green lines. The blue line shows the number of pairs of nearby soundings as a function of height.

indicates the number of pairs. The red line shows the mean difference; as expected, it is close to zero. The green lines show the standard deviations of the differences plotted around the mean. The standard deviations are smallest between about 8 and 20 km. This shows that the GPS RO observations have the highest precision in this altitude range, where the standard deviation is about 0.2% (e.g., equivalent to ~0.5°C in temperature). It is important to recognize that even with only a 10-km separation, there can still be significant real meteorological variability; this variability contributes to the standard deviations of the differences in pairs of soundings. In the lower troposphere, the standard deviation is larger, reaching 1% at 1 km. We suspect that this is related to RO retrieval errors resulting from uncorrelated noise between different occultations and considerably larger natural variability in the real atmosphere, primarily associated with small-scale variations in water vapor and clouds. The increase of the standard deviation above 20 km is most likely associated with the residual errors of the ionospheric calibration.

Next, to study the impact of atmospheric variability on the RO precision estimates, we define a Precision Parameter of the Upper Troposphere and Lower Stratosphere (PPUTLS), which is defined by the mean standard deviation of refractivity differences, expressed as a percent, between 10- and 20-km altitude. We stratify the PPUTLS as a function of tangent point separation distance and latitude. In Fig. 9 the value of 100 on the *x* axis means that the separation distance of pairs must be 100 km or less. We collected 533 pairs globally that have a separation distance of less than 5 km; for these pairs the PPUTLS value is 0.10%, which is equivalent to 0.25°C in temperature. Radiosondes typically have a precision of about 0.5°C (WMO 1996). Thus, the COSMIC RO observations globally are about two times more precise than radiosonde observations. One notices that the precision parameter increases rapidly as the tangent point separation increases from 1 to 5 km. This indicates that atmospheric turbulent motion and variability start to become significant. The PPUTLS stays at about 0.2% from 20 to about 100 km, and then increases steadily. This increase reflects the effects of mesoscale and synoptic-scale atmospheric variations.

If we compare the Northern with the Southern Hemisphere polar regions, we find that PPUTLS is higher in the Southern than in the Northern Hemisphere, particularly for tangent point separations of 200 km or greater. This is because these data were collected during the Northern Hemisphere summertime, and the winter (Southern) hemisphere tends to have more horizontal variability. These results show that the true atmospheric variability significantly affects the precision estimates when the two soundings are separated by a distance greater than about 100 km.

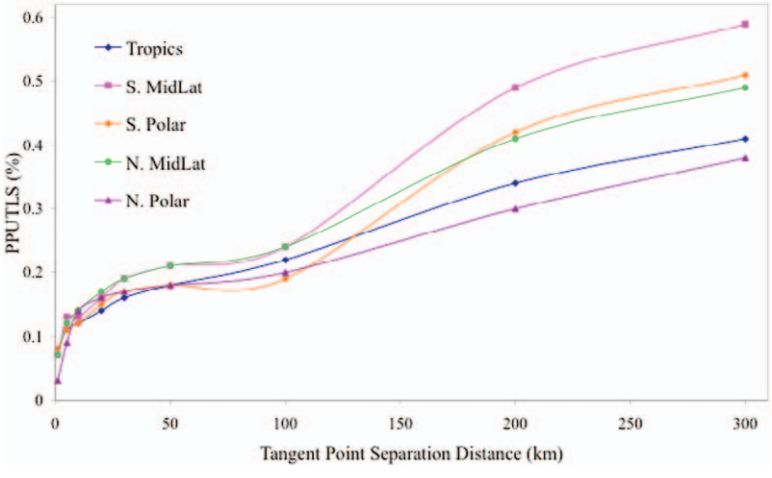

Fig. 9. The variation of the PPUTLS with latitude and tangent point separation distance.

FORECAST IMPACT AND ERROR STUDIES.

Impact on global forecast models. Several international centers are testing the impact of COSMIC data on operational NWP. ECMWF performed a data impact study by assimilating the COSMIC GPS RO bending angle profiles into the ECMWF operational NWP system from 14 September to 25 November 2006, using the observation operator described by Healy and Thépaut (2006). In a conservative approach, with the primary aim of reducing upper-tropospheric and stratospheric temperature errors, they used only data from setting occultations above 4 km. Nevertheless, COSMIC data produced a large, positive impact on stratospheric temperature forecasts in the Southern Hemisphere out to 10 days, even in the presence of all of the other data used operationally. Figure 10 shows fractional change in the root-mean-square (RMS) fit to radiosonde temperature measurements at 100 hPa in the Southern Hemisphere, over the day-1 to day-10 forecast range. The fractional change in the RMS is defined as $(1 - \mathrm{RMS}_{\mathrm{GPSRO}}/\mathrm{RMS}_{\mathrm{OPS}})$, where $\mathrm{RMS}_{\mathrm{OPS}}$ is the RMS fit achieved in operations (i.e., without GPS RO), and $\mathrm{RMS}_{\mathrm{GPSRO}}$ is the RMS fit when

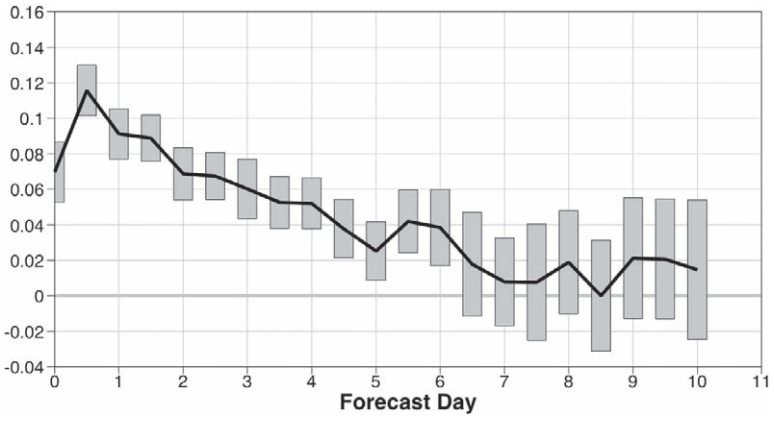

Fig. 10. Fractional reduction of 100-hPa RMS temperature errors in the Southern Hemisphere, verified against radiosonde observations, as a result of assimilation of COSMIC soundings. Positive values represent improvement in terms of RMS errors. The vertical bars represent the 95% confidence interval.

the COSMIC data are assimilated in addition to other observations. A positive value indicates a positive impact. The COSMIC data reduced the fractional 100-hPa temperature RMS errors by 11% for the 12-h forecasts over the Southern Hemisphere, which is an extremely large signal. The corresponding improvement in the standard deviation of the 12-h forecast errors was 5%, showing that assimilating the RO measurements reduced both the random and systematic temperature errors. Results over the tropics and Northern Hemisphere are also very encouraging. Based on these test results, ECMWF began using the COSMIC data (setting occultations only above 4 km) operationally on 12 December 2006. Currently, ECMWF is performing additional impact studies with COSMIC data from both setting and rising occultations down to the surface.

The National Oceanic and Atmospheric Administration/National Weather Service (NOAA/NWS) has developed, tested, and incorporated the necessary components to assimilate GPS RO profiles from the COSMIC mission into its next-generation NCEP Global Data Assimilation System. These components include different forward operators to simulate the observations from model variables and associated tangent linear and adjoint models, quality control algorithms, error characterization models, data-handling and data-decoding procedures, and verification and impact evaluation techniques (Cucurull et al. 2007). Recent impact studies have shown significant improvement on the anomaly correlation scores for the 500-hPa geopotential heights in both the Northern and Southern Hemispheres with the use of COSMIC data (Fig. 11).

In addition, a significant reduction of the stratospheric RMS error and bias in temperature is found for all latitudes when COSMIC profiles are used in the assimilation system. As a result of the positive impact of COSMIC on top of the observations used operationally, COSMIC data were incorporated into operations at NCEP, along with the implementation of the new Global Data Assimilation System [Gridpoint Statistical Interpolation/Global Forecast System (GSI/GFS)] on 1 May 2007.

Identification of errors in Antarctic regional model forecasts. Antarctica is a data-sparse region. Even though it is bigger than the continental United States, it has very limited surface and upper-air observations. In the summer, there are about a dozen radiosonde stations, mostly around the periphery of the continent, with one radiosonde station at the South Pole. In the winter, the number of radiosonde stations is reduced by half. Moreover, because it is permanently covered by snow and ice, the retrieval of satellite radiance observations is also very challenging and subject to significant uncertainties. As a result, models usually perform

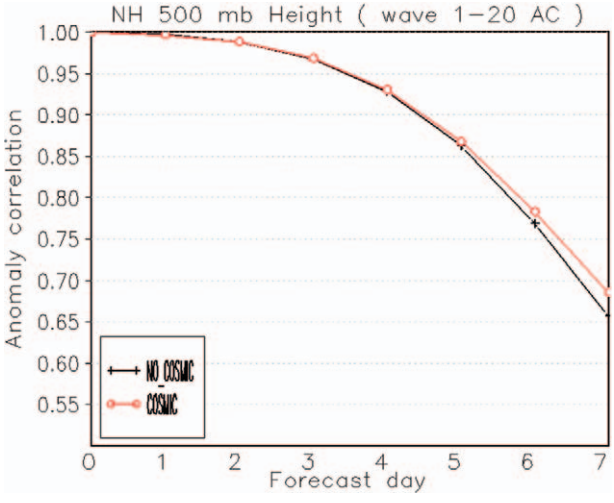

Fig. 11. Average anomaly correlation coefficients for 500-hPa forecasts in the Northern Hemisphere using the NCEP GFS system with and without the assimilation of COSMIC data for the month of Nov 2006. Both forecasts used all other observations normally used in the NCEP operational system for this month. The results are filtered to represent the structures with total wavenumbers 1–20.

poorly over this part of the world (Bromwich and Cassano 2000). Because of this lack of observations, we have only very limited knowledge of model performance and systematic biases. The COSMIC soundings provide an opportunity to evaluate state-of-the-art mesoscale models over the Antarctic. K. W. Manning and Y.-H. Kuo (2007, unpublished manuscript) used the COSMIC soundings collected during the period from 1 July to 1 September 2007 to evaluate the forecasts of the Weather Research and Forecasting (WRF) model, which is being tested for the implementation into the Antarctic Mesoscale Prediction System (AMPS; Powers et al. 2003). Figure 12 shows the WRF model's 48–60-h forecast error at 0.5 km above the surface in terms of refractivity, averaged for the period from 1 July to 1 September 2007. It is apparent that there was a systematic model error over the Antarctic and its surrounding area, with negative refractivity errors (except for the polar plateau over eastern Antarctica). According to Eq. (1), this implies that the model is systematically too warm over the Antarctic and its surrounding area at 500 m above the surface. A comparison with the sea ice coverage (Fig. 12, left) shows that the area with negative model refractivity errors corresponds very closely with that of the sea ice distribution. This close relationship suggests that the WRF model's treatment of the sea ice (and the stable ABL) requires improvement. We also note the substantial positive refractivity errors over the middle and subtropical latitudes on the outer edge of the model domain. The reasons are not yet known; however, they can be related to an overestimation in the prediction of water vapor over these regions. In any event, these results show that the COSMIC observations are useful for providing information on model errors.

Impact on forecasts of Tropical Storm Ernesto (2006). Tropical cyclones form and spend most of their life over tropical oceans, where observations of the moisture field assume critical importance in forecast models (Foley 1995). COSMIC observations provide information on the tropospheric moisture and temperature structure and, thus, have great potential to improve tropical cyclone predictions.

Y. Chen et al. (2007, unpublished manuscript) performed a set of 5-day numerical forecasts of Hurricane Ernesto (2006) using the WRF model. Ernesto originated from an easterly wave that exited Africa on 18 August 2006. Figure 13a shows an infrared satellite image of Ernesto at 0000 UTC 26 August as it moved into the central Caribbean Sea and intensified to tropical storm strength. In a forecast that did not use GPS observations, the WRF model was simply initialized from the NCEP GFS analysis at 0600 UTC

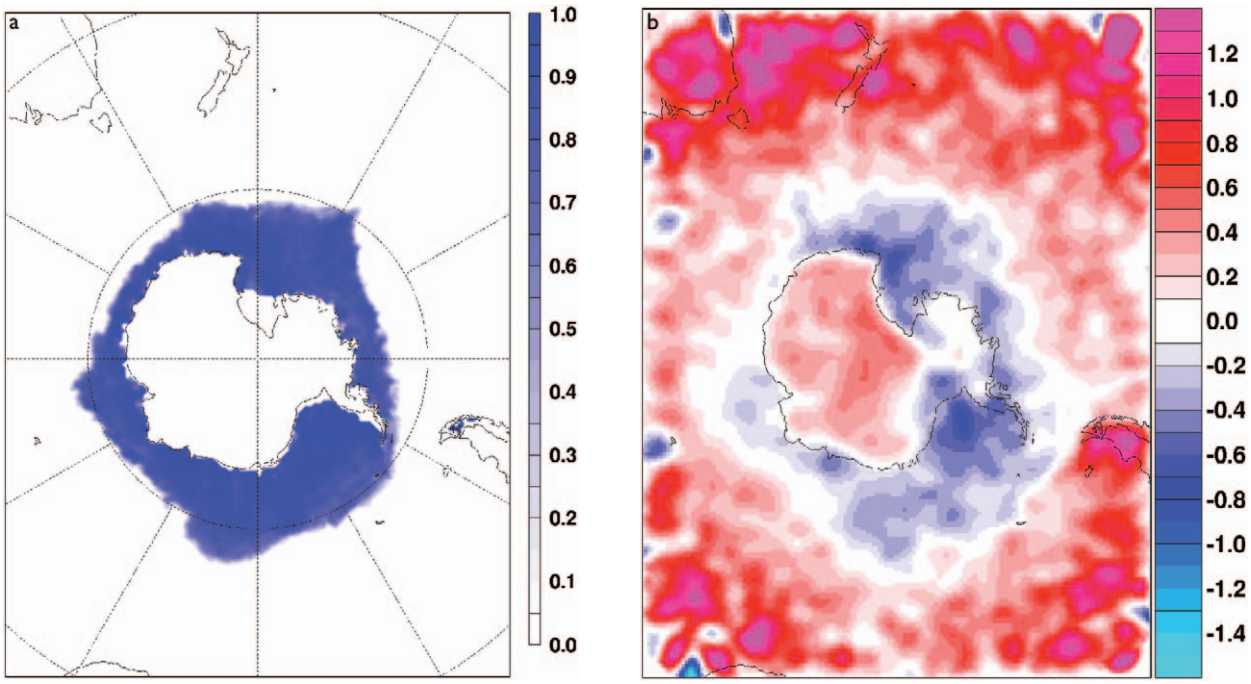

Fig. 12. (a) The sea ice (blue color) surrounding Antarctica for the period from 1 Jul through 1 Sep 2007; and (b) the WRF 48–60-h forecast refractivity errors at 0.5 km above the surface in units of refractivity, averaged during this period, as verified against COSMIC soundings. Negative errors (blue colors) are associated with ice and positive errors (red colors) are over open water and land.

23 August to produce a 5-day forecast. In the GPS experiment, 15 COSMIC RO soundings collected during a 6-h period from 0300 to 0900 UTC 23 August were assimilated into the initial fields using a deterministic ensemble filter (Anderson 2001) that are part of NCAR's community Data Assimilation Research Testbed facility (online at www.image.ucar.edu/DAReS/DART/). A 5-day deterministic forecast was then initialized from the updated ensemble mean analysis. The 66-h forecasts of the vertically integrated total cloud water mixing ratio (plotted in logarithm scale for comparison with the infrared satellite image) from the two experiments are shown in Figs. 13b and 13c. Without assimilation of COSMIC data, the model failed to develop organized convection from the beginning, and no tropical storm appeared in the model throughout the 5-day forecast period. Assimilating COSMIC soundings moistened the lower troposphere in the area of organized convection. The hurricane genesis process was simulated and Tropical Storm Ernesto developed in the model following that of the observed storm. Similar results were obtained in a 2-week-long GPS RO assimilation experiment by H. Liu et al. (2007, unpublished manuscript). These results indicate that GPS RO data may be useful in improving numerical forecasts of tropical cyclone genesis.

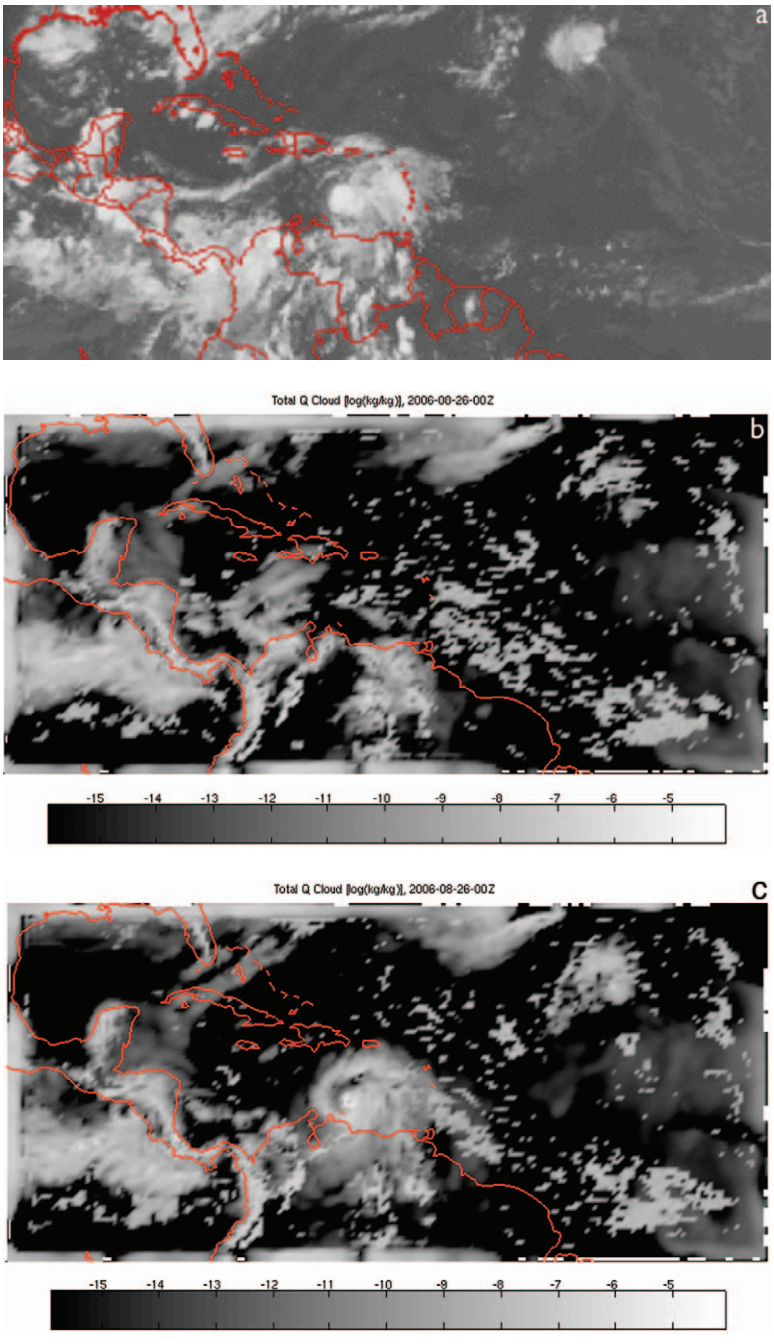

Fig. 13. (a) Infrared satellite photo for 0000 UTC 26 Aug 2006. Tropical Storm Ernesto is located near the center between South America and Puerto Rico. (b) Vertically integrated cloud water mixing ratio for the no GPS experiment, which only uses the NCEP global analysis as the initial conditions. This is a 66-h forecast. (c) Same as in (b), but with assimilation of 15 COSMIC soundings.

CLIMATE APPLICATIONS.

Radio-occultation observations are well suited for establishing a stable, long-term record required for climate monitoring (Goody et al. 1998; Mannucci et al. 2006). In spite of the enormous importance of detecting climate trends, there is presently no atmospheric instrument that can meet the stringent climate monitoring requirements of 0.5-K accuracy and 0.04 K decade^{-1} stability (Ohring et al. 2005).

Because the fundamental observation is a measurement of time, RO is a promising technique for climate monitoring. Atomic clocks can measure time with unequaled accuracy and stability. During an occultation, the GPS receiver measures the change in the flight time of the signal transmitted by the occulted GPS satellite. The clocks aboard the GPS

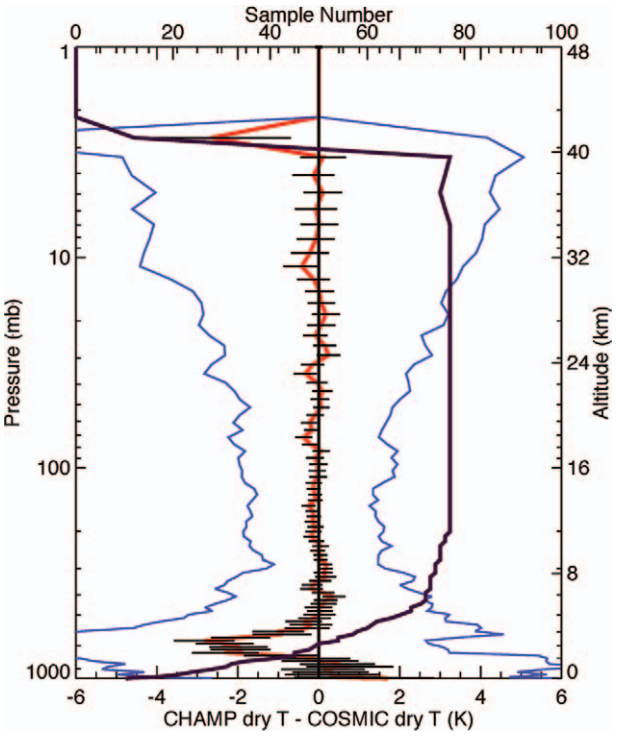

Fig. 14. Comparison statistics (mean: red; standard error of the mean: horizontal black lines superimposed on the mean; std dev: blue; sample number of compared soundings: solid black line) of 80 CHAMP and COSMIC profiles that were collocated within 200 km and 90 min from 1 Sep to 31 Oct 2006, within 60°S–60°N.

transmitters remain synchronized to the most stable atomic clocks on the ground. The clock in the GPS receiver on the COSMIC low-Earth orbiter (LEO) is synchronized, using the signals from up to 10 nonocculted GPS transmitters in view and is thus tied to the stable ground-based GPS time as well. Therefore, an extremely accurate measurement of the signal flight time with long-term stability can be achieved. From this time measurement we compute the delay caused by the neutral atmosphere, and from this delay atmospheric profiles are derived. These profiles are theoretically expected to have the accuracy and stability required for climate applications. They are also expected to be mission independent, implying that results from COSMIC, or any RO mission, can be compared directly to results from RO missions launched many decades from now.

Comparison of GPS RO soundings from different missions. For verification of the claim of mission independence we compared profiles from the COSMIC and CHAMP missions. Figure 14 (based on Fig. 7 in Ho et al. 2008) shows such a comparison for 80 pairs of "dry temperature" profiles that were obtained within 200 km and 1.5 h of each other in September and October 2006, but within 60°S–60°N. Although the data sample is not large, the results show that the mean temperature difference in the height range from 5 to 40 km is not significantly different from zero (as indicated by the standard error of the mean difference).[3] These results support the claim of mission independence of RO temperature soundings in the 5–40-km height range.

Figure 15 shows a time series of temperature anomalies at 100 hPa for a subtropical latitude band of 20°–30°S from multiple missions, including SAC-C, CHAMP, and COSMIC. The temperature anomalies were computed by subtracting the monthly averages (computed for the entire 5.5-yr span) from the individual RO temperature measurements of the corresponding months. Figure 15 shows that there is no obvious change or jump in temperature anomalies between the missions, for example, when the COSMIC observations are added in 2006. This result supports the expectation that the properties of different RO observations are consistent and independent of mission, as was also shown in Fig. 14.

The COSMIC constellation, after full deployment into six orbital planes separated by 30°, continuously sample all local times. This is especially important for establishing a climate record, because it largely eliminates aliasing of the diurnal cycle and removes diurnal cycle biases.

While the expectations for RO as a global climate-monitoring technique are high, there are several issues that still require further investigation to ensure that all systematic errors are fully understood. Computing the delay caused by the neutral atmosphere requires that we know the geometric distance between the LEO and the GPS satellite, and especially its rate of change, very accurately. Accurate orbit estimation and good knowledge of the receiving and transmitting antenna phase patterns are required. Furthermore, the ionospheric effect on the signal delay must be corrected. This is done by use of the dual-frequency GPS data (Kuo et al. 2004). Both the orbit determination and the ionospheric correction have errors. A careful analysis of these and other errors was presented by Kursinski et al. (1997). We presently expect that with state-of-the-art data processing, all errors affecting RO can

[3] The significant differences between CHAMP and COSMIC "dry" temperatures below 5 km are consistent with the differences between CHAMP and COSMIC refractivities discussed in section 2a (Fig. 2). Also, the number of comparisons substantially decreases below 5 km, so contribution of the sampling errors may not be insignificant.

be kept below the 0.5-K accuracy and 0.04 K decade^{-1} stability level in the height range of 8–25 km above the surface. Below about 8 km (this height depends on latitude), the effect of atmospheric water vapor complicates the use of the observations for climate research. Above 25 km, residual ionospheric and small systematic orbit determination errors can, while still entirely acceptable for use in weather models, introduce RO profile errors that may exceed the strict climate monitoring requirements.

Comparison of GPS RO soundings with AMSU measurement. While RO observations will establish a climate record by themselves, they can also be very useful for assessing the quality of the observations from other sensors, like the Microwave Sounding Unit (MSU) and Advanced Microwave Sounding Unit (AMSU) in the 8–25-km height range. For example, Ho et al. (2007) found that MSU/AMSU from both Remote Sensing System, Inc. (RSS), and University of Alabama at Huntsville (UAH) channel 4 stratospheric retrievals in the Antarctic lower stratosphere in winter were biased high relative to temperatures derived from GPS RO measurements.

Accurate, consistent, and stable observations from different satellites are crucial for climate change detection. However, even with accurate prelaunch calibrations in laboratories against known sources of radiant energy, MSU and AMSU instrument characterization may still change after launch because of strong vibration during the launch and the extreme environment in orbit. Even with continuous on-orbit calibration for each satellite instrument, on-orbit drift errors and intersatellite biases are still obvious (Karl et al. 2006). The processing assumptions by different groups (e.g., Christy et al. 2003; Mears et al. 2003), along with the inadequacies in the observations, result in structural uncertainties that contribute to differences in the temperature records in the stratosphere and troposphere and between surface and tropospheric temperature trends. To construct consistent datasets from different satellite missions, we need to have an independent dataset free of on-orbit drift errors and satellite-to-satellite biases to intercalibrate measurements from different satellite missions (Trenberth et al. 2006).

To demonstrate the usefulness of COSMIC data to intercalibrate measurements from similar instruments but on different satellites, we convert COSMIC temperatures to equivalent AMSU channel 9 brightness temperatures (Tb) and compare these to the AMSU Tb from *NOAA-15* (*N15*) and *NOAA-18* (*N18*). The contribution of AMSU channel 9 is mainly from the upper troposphere to the lower stratosphere (peak at 110 hPa). COSMIC temperature profiles are provided as input to an AMSU forward model to obtain the COSMIC-equivalent Tb. The comparisons are shown in Fig. 16 (based on Fig. 5 of Ho et al. 2008). The collocated AMSU Tb *N15* and *N18* occur within 30 min and 0.5° latitude of the COSMIC soundings. Figure 16 shows that synthetic COSMIC Tb is highly correlated with that from both *N15* (correlation coefficient 0.99) and *N18* (correlation coefficient 0.998), and with small standard deviations to the means of COSMIC–*N15* (0.97 K) and COSMIC–*N18* (0.95 K), respectively. However, because *N15* and *N18* are on different orbits, the shift of sensor temperature owing to on-orbit heating/cooling of satellite components (Christy et al. 2003) varies, and there are intersatellite offsets that can be identified by the COSMIC Tb. The

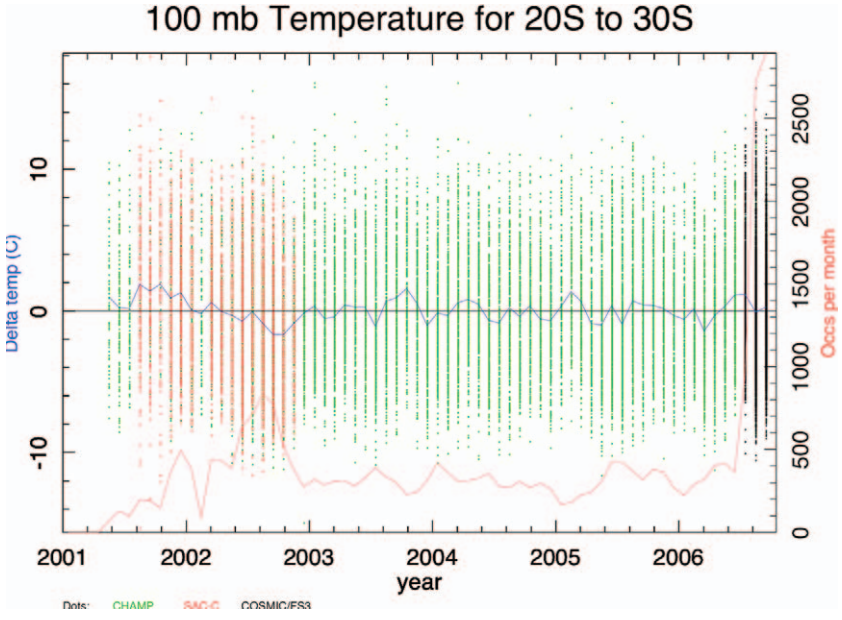

Fig. 15. The RO temperature record from three missions. The vertical lines are composed of dots representing individual soundings, CHAMP (green), SAC-C (red), and COSMIC (black) minus the overall monthly average temperature. The average temperature for a given month minus the average for that month over the entire time series (blue line) and the total number of occultations per month (red line) are shown.

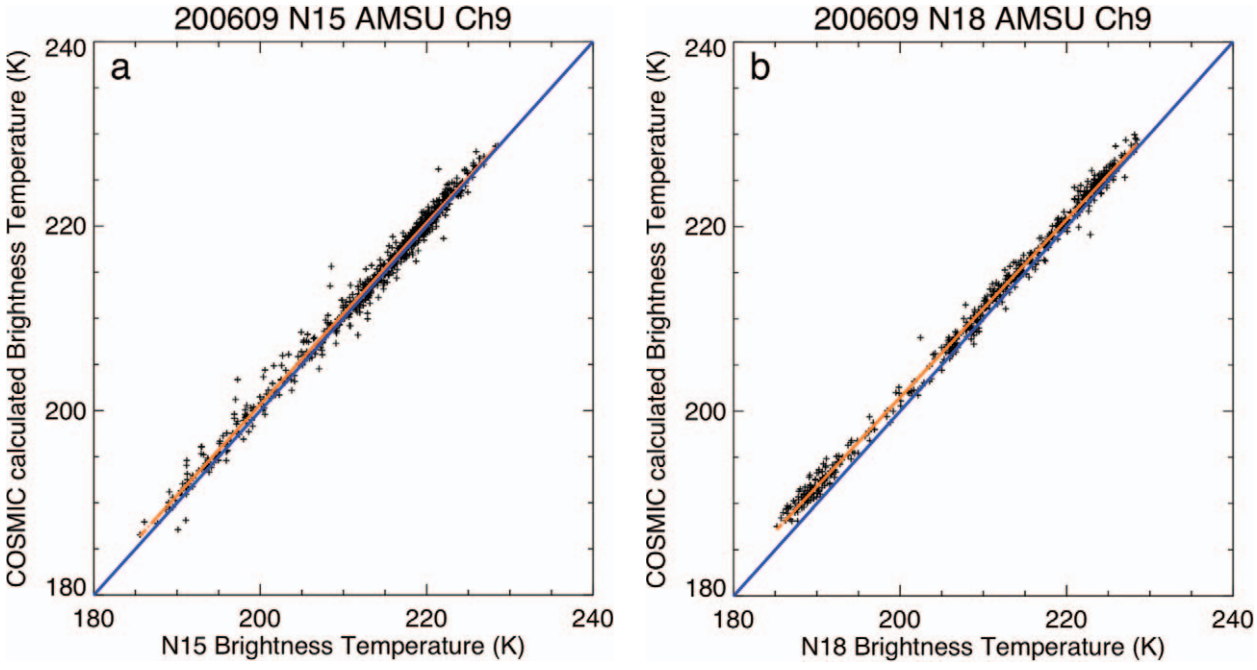

Fig. 16. Comparison of COSMIC-simulated AMSU Ch9 Tbs and (a) *NOAA-15* AMSU Ch9 Tbs and (b) *NOAA-18* AMSU Ch9 Tbs for Sep 2006.

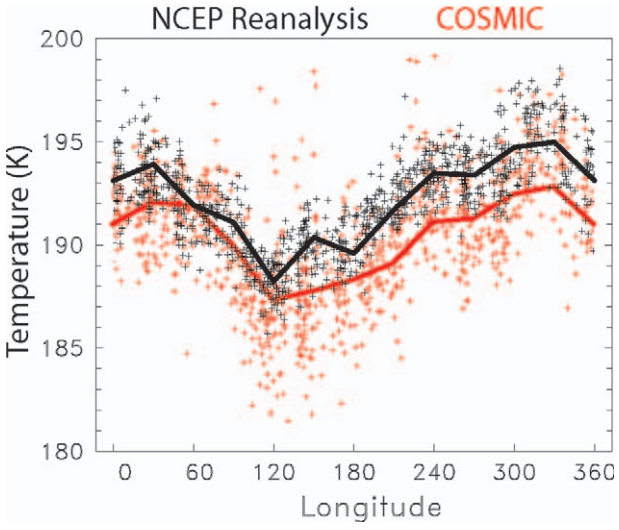

Fig. 17. Temperatures (red +) at the cold-point tropopause derived from all COSMIC temperature retrievals over 10°N–S for 20–30 Dec 2006. Each point represents one sounding, and the red line indicates the average longitudinal structure. The black line denotes the cold-point tropopause average derived from NCEP reanalysis data for the same time period, with individual points (black +) sampled identically to the COSMIC data.

tight fit of COSMIC Tb to *N15* and *N18* Tb demonstrates the usefulness of COSMIC data to calibrate, in this case, both *N15* and *N18,* which suffer from different orbit-drift effects and sensor sensitivity decay of the AMSU instruments with time. The uniform global and temporal coverage from COSMIC after its final deployment allows intercalibration of microwave and infrared satellite data from both LEO and geostationary satellites against COSMIC data.

Observations of the tropopause. The global tropopause has received considerable attention for problems in dynamic meteorology and stratosphere–troposphere coupling, and for potential as an indicator of climate variability and change (Santer et al. 2003; Seidel and Randel 2006). The accurate, high vertical resolution temperature profiles from RO afford a unique opportunity to observe tropopause structure and variability, and COSMIC is providing this information on a global scale (with a substantially higher resolution and global coverage than is available with other data). As an example, Fig. 17 shows the temperature of the tropical cold-point tropopause during 20–30 December 2006, derived from COSMIC occultations over 10°N–10°S, and includes a comparison of the same diagnostic calculated from NCEP–NCAR reanalysis data (Kalnay et al. 1996). Both datasets show the well-known structure of tropopause temperature minima over the Indonesian region, overlying the area of the strongest tropical convection (Highwood and Hoskins 1998). There is an overall warm bias to the NCEP results, primarily because of the lower vertical resolution of the analyses in the region of the sharp cold point. However, beyond this mean difference, the COSMIC data show substantially enhanced variability in the

individual measurements compared to that of the NCEP data. Previous analyses of tropical RO data have shown that this variability is realistic and associated with large- and small-scale waves near the tropical tropopause, tied to transient tropical convection (Randel et al. 2003; Randel and Wu 2005). Capturing this variability is key for understanding problems such as dehydration and cirrus cloud formation near the tropopause (Jensen and Pfister 2004), and for understanding the impact of deep convection on the tropopause region. The resolution and sampling of COSMIC provide a novel tool for monitoring tropopause variability, quantifying the relevant physical mechanisms, and measuring potential long-term changes.

IONOSPHERIC RESEARCH AND SPACE WEATHER. The GPS receivers on board the COSMIC satellites also generate a massive amount of ionospheric data that are inverted into vertical electron density profiles and total electron content (TEC) along GPS–COSMIC radio links. These data, together with the complementary TIP and TBB data, are valuable for evaluation of ionospheric models and use in space weather data assimilation systems.

Electron density profiles and total electron content. The RO electron density profiles from COSMIC are processed as described in Schreiner et al. (1999), Syndergaard et al. (2006), and Lei et al. (2007). Lei et al. (2007) also show some of the first comparisons made between COSMIC-derived electron density profiles and those measured by incoherent scatter radars (ISR) at Millstone Hill in Massachusetts and Jicamarca in Peru. Generally, the COSMIC profiles agree well with the ISR measurements. During the first few months of the mission, COSMIC generated many collocated ionospheric profiles that have been used to establish the precision of RO measurements in the ionosphere (Schreiner et al. 2007). As the satellites slowly spread apart, they provided a unique opportunity for studies of ionospheric variability from space. As an example, Fig. 18 shows the retrievals of five electron density profiles from five different COSMIC satellites at times when the satellites were closely following each other. The five occultations happened within several minutes of each other around local noon at the northwest slope of the northern crest of the equatorial anomaly. The occultations of *FM3* and *FM4* happened almost at the same place and time. The retrieved profiles from these two occultations are nearly identical and serve as an example of the high degree of repeatability of the GPS ionospheric measurements from different platforms. The profiles measured at four different times exhibit an increase in the height of the peak density as time progresses, and also a shift in location toward lower latitudes. It is not clear whether the change in peak height is a true temporal effect or merely a result of the slightly different locations of observations. One possible way to separate the temporal and spatial effects in the COSMIC occultation data is to compare the vertical information from RO with the data from the two other COSMIC instruments, TIP and TBB. These instruments can be used to locate horizontal structures such as traveling ionospheric disturbances (TIDs) and ambient density gradients at night and over TBB ground stations. The nonzero values of electron density below 80-km altitude in Fig. 18 (where the density in theory should be almost zero) give an

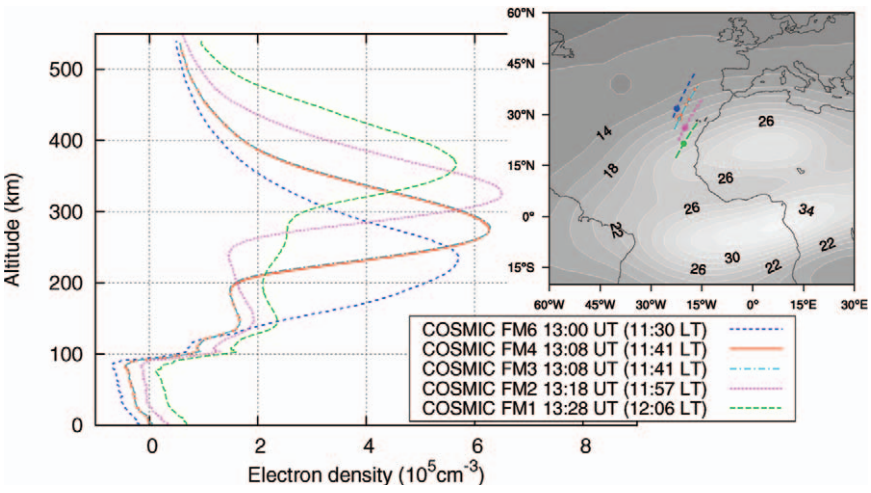

Fig. 18. Five profiles of electron density measured on 26 Aug 2006. The five GPS occultations are observed minutes apart by five different COSMIC satellites flying in almost identical orbit planes while receiving signals from the same GPS satellite (PRN 14). The insert map shows the locations of the occultations as well as the contours of the vertical TEC (10^{16} m^{-2}) at 1330 UTC obtained from the Jet Propulsion Laboratory high-resolution global ionospheric maps. The colored lines on the map indicate the tangent point trajectories for the occultations and the dot on each trajectory indicates the location where the tangent point altitude is at the F peak of each profile.

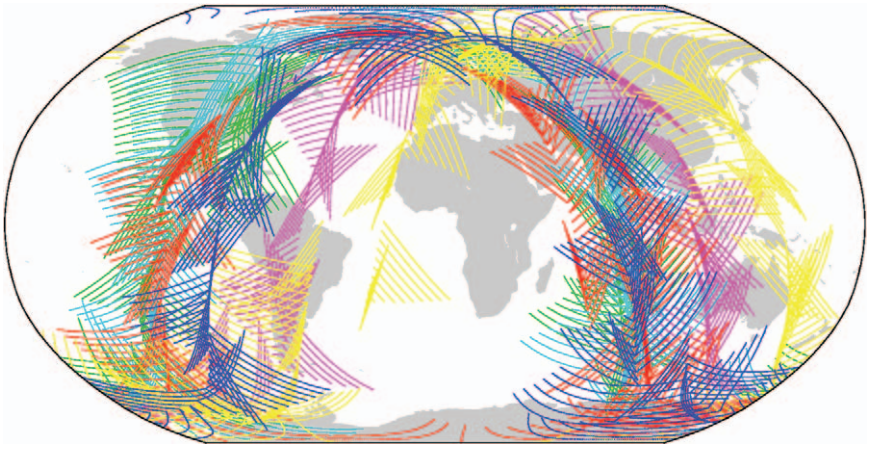

Fig. 19. GPS–COSMIC transionospheric radio links below COSMIC orbit altitudes for a period of 100 min (approximately one orbit revolution for each satellite) centered on 1400 UTC 4 Mar 2007. Adjacent links within the same occultation are plotted one minute apart although the data are sampled at 1 Hz. The colors indicate the same COSMIC *FM* numbers as in Fig. 18, but with the addition of *FM-5* (yellow).

indication of the uncertainty of the profile retrievals. This uncertainty is caused by horizontal gradients not presently taken into account in the inversion of the occultation data.

Dual-frequency GPS observations can be used to determine TEC (Hajj et al. 2000). The measurements of TEC along GPS–COSMIC links are potentially valuable for data assimilation into ionospheric models, like the JPL/University of Southern California Global Assimilative Ionospheric Model (JPL/USC GAIM) (Wang et al. 2004) and the Utah State University Global Assimilation of Ionospheric Measurement model (USU GAIM) (Schunk et al. 2004). Figure 19 shows the GPS–COSMIC transionospheric radio links (i.e., radio links with negative elevation angles relative to the horizontal) for a period of just 100 min on 4 March 2007. In addition to the negative elevation angle measurements, COSMIC also measures the TEC at positive elevation angles up to 90° on the aft antennas and up to 30° on the forward antennas. As the satellites moved into their final orbits at 800 km by the end of 2007, the global coverage within a 100-min period became more uniform. Many research groups running space weather models have begun to assimilate the TEC data. Early results have been presented at various scientific meetings, and publications are expected in the near future.

Figure 20 shows a comparison of COSMIC-retrieved electron density with that of the USU Gauss–Markov GAIM (Scherliess et al. 2006). For the comparison of the peak electron density at the F2 layer, the correlation coefficient is as high as 0.92. However, the corresponding correlation coefficient for the comparison of the height of the peak electron density is only 0.6. In general, we find that the USU GAIM shows a systematic high bias for the height of the F2 peak electron density. This is understandable, because most of the ionospheric observations (e.g., from ground-based GPS receivers) that were assimilated by GAIM for this study do not contain much vertical gradient information, and therefore, the height is reflecting the underlying ionospheric model. These results clearly show that the COSMIC data will be very useful for improving ionospheric data assimilation and forecast modeling and will make a significant contribution to space weather studies.

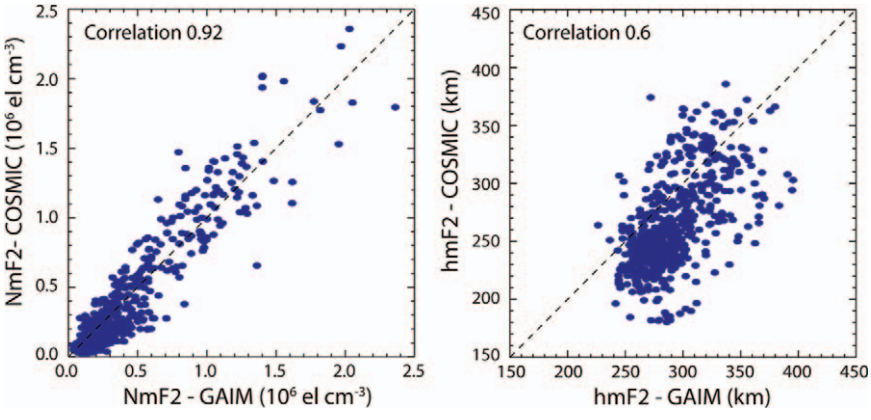

Fig. 20. Comparison of COSMIC-retrieved electron density with that of the USU Gauss–Markov GAIM model. The left panel shows the peak electron density (NmF2) of COSMIC profiles compared with the GAIM peak electron density taken at the location where the tangent point altitude is at the F peak of each COSMIC profile. The right panel shows a comparison of the corresponding peak heights (hmF2). The data were collected during the first week of COSMIC measurements (21–28 Apr 2006).

TIP and TBB measurements. The TIP and TBB payloads on COSMIC are also providing exciting new data. Figure 21 shows an example of TIP observations (Dymond et al. 2000). The TIP observes the ionosphere only at night, because the day airglow is contaminated by molecular emissions that are not of ionospheric origin. Global scans of 1356-Å radiation, produced by the natural decay of the ionosphere by recombination of ions and electrons, show the equatorial anomaly arcs, which are represented by the green- to red-colored traces. The thin line across the image indicates the geomagnetic equator. The equatorial arcs are symmetrically distributed about the magnetic equator. The separation of the arcs is determined by the strength of the daytime eastward electric field and the zonal wind field near 100-km altitude. The changing separation seen in the figure is an indicator of the variability of the electric field and zonal wind fields that drive ionospheric dynamics. Latitudinal variations in the intensity of the arcs are driven by the presence of meridional thermospheric winds. The variation of the arc intensities with longitude is a good indicator of the variability of the meridional wind field. Additionally, the TIP data show the presence of the ionospheric depletions (sharply decreasing intensities) associated with equatorial spread F or radio frequency scintillation. Regions showing depletions are indicated in Fig. 21. The TIP instruments directly measure the horizontal electron density gradient. This gradient information can be used to correct the GPS RO retrievals, in regions where the electron density gradient is large, to produce more accurate electron density profiles (Dymond et al. 2000).

The CERTO TBB on COSMIC is used to transmit signals to ground-based receivers (Bernhardt et al. 2000; Bernhardt and Siefring 2006) and to a receiver in low-Earth orbit (Bernhardt et al. 2006). Ionospheric-relative TEC along COSMIC to ground links is determined from the differences in the phase between the VHF (150.012 MHz) and UHF (400.032 MHz) frequencies of the CERTO TBB with a typical precision of 0.05 10^{16} m^{-2}. The VHF and UHF frequencies plus the L-band frequency (1,066.752 MHz) are used to measure ionospheric radio scintillations by monitoring phase and amplitude variations at the receiver. A chain of receivers deployed along the east coast of Asia through Taiwan has been receiving COSMIC TBB signals and providing TEC and scintillation data since its launch. Another established north–south chain in Alaska has also been recording TEC data from COSMIC. Since late 2006, receivers were set up at Lima, Peru; Arecibo, Puerto Rico; New York; Massachusetts; Texas; Florida; and other locations in both South and North America. On 8 March 2007, the Naval Research Laboratory's Computerized Ionospheric Scintillation and Tomography Receiver in Space (CITRIS) was launched into a 560-km-altitude orbit with a 35° inclination. CITRIS is designed to receive the COSMIC TBB signals for satellite-to-satellite measurements of ionospheric TEC and radio scintillations (Bernhardt and Siefring 2006; Bernhardt et al. 2006).

Samples of the line-of-sight TEC from the COSMIC satellites to a ground station are shown in Fig. 22. The data for this figure were obtained at night from the Patrick Air Force Base in Florida using a CERTO beacon receiver provided by the U.S. Air Force as part of the network that supports the RADCAL, GFO, and DMSP/F15 satellites. As the COSMIC satellite passes over the ground receiver, horizon-to-horizon measurements of the TEC are obtained.

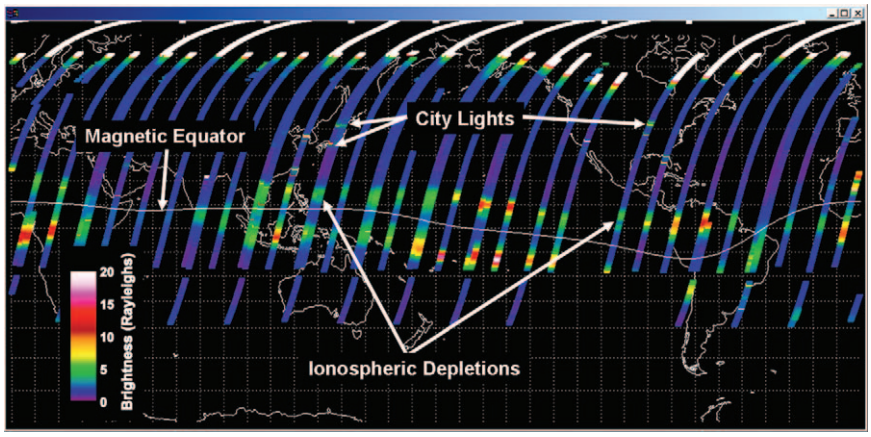

Fig. 21. Global scans of the 1356 Å radiation from the TIP instruments. TIP data are collected only on the night side. The magnetic equator is the wavy white line passing across the middle of the figure. The equatorial anomaly arcs can be seen as the green–red colored traces symmetrically distributed about the magnetic equator. Two regions showing ionospheric density depletions (intensity sharply decreases) associated with radio frequency scintillation are visible. The TIP instruments show some sensitivity to city lights; for example, the small-scale increases in intensity (indicated in figure) correspond with the locations of large cities.

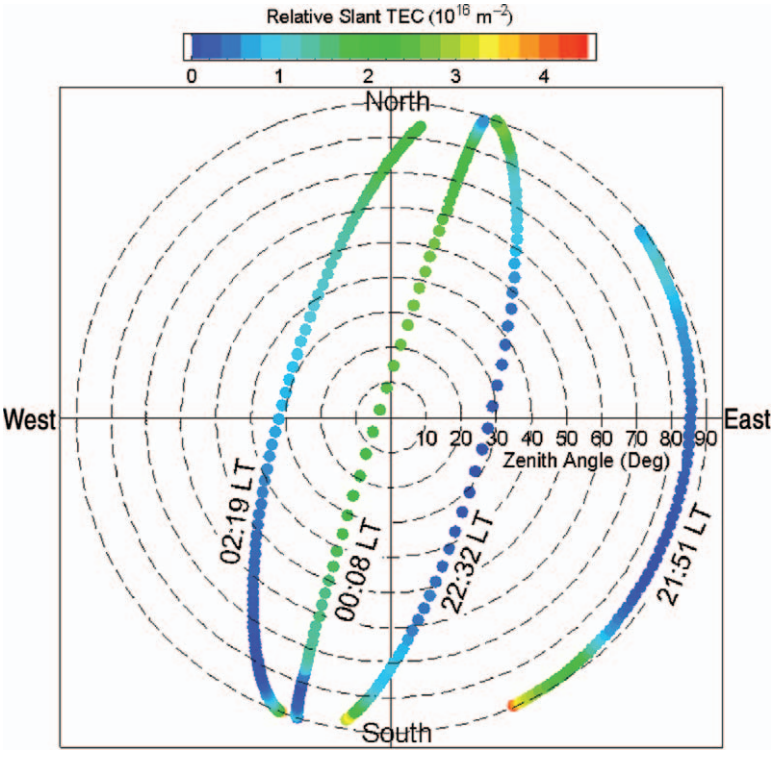

FIG. 22. Samples of relative (with respect to the smallest observed value), slant-path TEC data from Patrick AFB, Florida, based on CERTO–TBB transmissions at 150.012 and 400.032 MHz from COSMIC *FM-1, FM-5,* and *FM-6*. The data were taken on 21 Dec 2006, from 0251 to 0719 UTC. The position of the satellite relative to the ground station is displayed in terms of azimuth and zenith angle. The TEC data are taken near 0000 LT when the variations in slant TEC show irregular structures.

The blue regions to the east before midnight and to the south near midnight outline regions of extremely low relative TEC. Several ionospheric campaigns that involve CERTO beacon signals from COSMIC were conducted in late 2006 organized by the Air Force Research Laboratory. These and other COSMIC TBB data will be incorporated with COSMIC TEC data from the GPS receivers to improve electron density profiles (Bernhardt 2005). In addition, the nighttime ionosphere will be investigated with the COSMIC CERTO/TBB and TIP instruments to provide cross-calibration and high-resolution (10 km) multinstrument tomography (Dymond et al. 2006).

SUMMARY AND CONCLUSIONS. The joint Taiwan–U.S. COSMIC/FORMOSAT-3 mission is providing a powerful demonstration of radio occultation, in particular, and of the remote-sensing applications of microsatellite constellations in general. Currently (September 2007), about 2,000 high-quality soundings are being retrieved daily on a global basis. These data are being provided to global weather prediction centers in near–real time and are being tested for their impact on weather forecasts. The data are available to researchers free of charge, and over 480 scientists from all over the world have registered to use the data.

The RO soundings using a new open-loop (OL)-tracking technique in the troposphere are significantly improved over previous soundings from satellites using the phase-locked loop (PLL) technique. The negative refractivity bias in the lower troposphere present in earlier RO missions using PLL tracking is significantly reduced, and the fraction of soundings reaching to within 1 km of Earth's surface is greatly increased. We estimate conservatively that about 70% of the COSMIC soundings penetrate below 1 km over the sea surface in the tropics, with about 90% reaching this depth in high latitudes. This is not a fundamental limit of the RO technique, and it is expected to be improved in the future. The OL technique also permits rising as well as setting occultations. For the first time, RO has shown a consistent ability to profile the vertical structure of the atmospheric boundary layer.

During the first few months after launch, several of the satellites orbited within a few tens of kilometers of each other. This afforded an unprecedented opportunity to compare RO soundings from different platforms and instruments. These comparisons have verified the expected high precision of RO soundings; the precision of individual profiles in the upper troposphere/lower stratosphere is equivalent to about 0.05°C.

The RO observations have already shown a significant, positive impact on the global forecasts; significant, positive impacts on individual forecasts of tropical cyclones; and identified systematic errors in model forecasts over the Antarctica. The COSMIC observations have supported the claims of high-precision, unbiased, and consistent (repeatable) observations from different instruments, platforms, and missions, all of which are important characteristics for producing accurate and stable long-term climate data records. Consequently, the potential

exists for COSMIC and other RO data to calibrate the climate record in the free atmosphere.

COSMIC data have been compared to data from the Advanced Microwave Sounding Unit (AMSU) from *NOAA-15* and *NOAA-18*. We find that the COSMIC and AMSU data are highly correlated (~0.99 or higher) with standard deviations to the mean between 0.95 and 0.97. The COSMIC data are capable of identifying intersatellite offsets between *NOAA-15* and *NOAA-18*, which demonstrate the value of RO observations in the intercalibration of satellite data.

The COSMIC mission has generated many ionospheric vertical profiles of electron density and total electron content (TEC) along COSMIC–GPS links. The ionospheric profiles have already been compared to ground-based data and show potential for studying ionospheric gradients and dynamics. The profiles are also useful in evaluating ionospheric models and data assimilation systems. It is anticipated that the TEC data will soon be assimilated into space weather models on a regular basis.

The other two instruments on the COSMIC satellites, TIP and TBB, are also providing exciting new observations. The TIP instrument is routinely collecting data at night, and observes the equatorial anomaly arcs and other density anomalies through measurements of 1356-Å radiation. The TBB enables observations from the line-of-sight TEC and scintillations between the COSMIC satellites and ground stations. The data from these instruments complement the ionospheric observations from the GPS receivers and could be used to improve the retrieval of electron density profiles at night and over TBB ground stations.

All in all, the results from the COSMIC mission are exceeding expectations. We look forward to many more scientific results as researchers around the world explore the power of these observations.

ACKNOWLEDGMENTS. Many people, too numerous to mention, contributed over the past decade to the COSMIC mission. We thank the National Space Organization and National Science Council in Taiwan for their primary sponsorship of the mission. We thank Jay Fein of the National Science Foundation for his leadership role throughout the project. COSMIC is sponsored in the United States by NSF, NASA, NOAA, the Air Force Office of Scientific Research, the Office of Naval Research, and the Space Test Program. We acknowledge especially NASA and JPL for their leadership role in providing the GPS receivers and associated firmware, and for radio-occultation science, in general. The work presented in this paper has been supported in part by a number of NSF grants, including NSF/ATM-0410014, NSF/ATM-9908671, NSF/INT-0129369, NSF/OPP-0230361.

REFERENCES

Anderson, J. L., 2001: An ensemble adjustment Kalman filter for data assimilation. *Mon. Wea. Rev.,* **129,** 2884–2903.

Anthes, R. A., 2006: COSMIC away! *UCAR Quarterly,* Spring 2006, 2–3. [Available online at www.ucar.edu/communications/quarterly/spring06/president.jsp.]

Ao, C. O., T. K. Meehan, G. A. Hajj, A. J. Mannucci, and G. Beyerle, 2003: Lower troposphere refractivity bias in GPS occultation retrievals. *J. Geophys. Res.,* **108,** 4577, doi:10.1029/2002RS002800.

Bernhardt, P. A., 2005: Eye on the ionosphere. *GPS Solutions,* **9,** 174–177.

——, C. L. Siefring, 2006: New satellite-based systems for ionospheric tomography and scintillation region imaging. *Radio Sci.,* **41,** RS5S23, doi:10.1029/2005RS003360.

——, C. Selcher, S. Basu, G. Bust, and S. C. Reising, 2000: Atmospheric studies with the Tri-Band Beacon instrument on the COSMIC constellation. *Terr. Atmos. Oceanic Sci.,* **11,** 291–312.

——, C. L. Siefring, I. J. Galysh, T. F. Rodilosso, D. E. Koch, T. L. MacDonald, M. R. Wilkens, and G. Paul Landis, 2006: Ionospheric applications of the scintillation and tomography receiver in space (CITRIS) used with the DORIS radio beacon network. *J. Geodesy,* **80,** 473–485.

Beyerle, G., T. Schmidt, J. Wickert, S. Heise, M. Rothacher, G. König-Langlo, and K. B. Lauritzen, 2006: Observations and simulations of receiver-induced refractivity biases in GPS radio occultation. *J. Geophys. Res.,* **111,** D12101, doi:10.1029/2005JD006673.

Bromwich, D. H., and J. J. Cassano, 2000: Recommendations to the National Science Foundation from the Antarctic Weather Forecasting Workshop, BPRC Miscellaneous Series M-420, 48 pp. [Available from Byrd Polar Research Center, The Ohio State University, 1090 Carmack Rd., Columbus, OH 43210-1002.]

Cheng, C.-Z., Y.-H. Kuo, R. A. Anthes, and L. Wu, 2006: Satellite constellation monitors global and space weather. *Eos, Trans. Amer. Geophys. Union,* **87,** 166–167.

Christy, J. R., R. W. Spencer, W. B. Norris, W. D. Braswell, and D. E. Parker, 2003: Error estimates of Version 5.0 of MSU/AMSU bulk atmospheric temperatures. *J. Atmos. Oceanic Technol.,* **20,** 613–629.

Cucurull, L., J. C. Derber, R. Treadon, and R. J. Purser, 2007: Assimilation of Global Positioning System radio occultation observations into NCEP's Global Data Assimilation System. *Mon. Wea. Rev.,* **135,** 3174–3193.

Dymond, K. F., J. B. Nee, and R. J. Thomas, 2000: The tiny ionospheric photometer: An instrument for measuring ionospheric gradients for the COSMIC constellation. *Terr. Atmos. Oceanic Sci.,* **11,** 273–290.

——, S. E. McDonald, C. Coker, P. A. Bernhardt, and C. A. Selcher, 2006: Simultaneous inversion of total electron content and UV radiance data to produce F region electron densities. *Radio Sci.,* **41,** RS6S19, doi:10.1029/2005RS003363.

Foley, G., 1995: Observations and analysis of tropical cyclones. Global Perspective on Tropical Cyclones, WMO/TD 693, 1–20.

Goody, R., J. Anderson, and G. North, 1998: Testing climate models: An approach. *Bull. Amer. Meteor. Soc.,* **79,** 2541–2549.

Gorbunov, M. E., H.-H. Benzon, A. S. Jensen, M. S. Lohmann, and A. S. Nielsen, 2004: Comparative analysis of radio occultation processing approaches based on Fourier integral operators. *Radio Sci.,* **39,** RS6004, doi:10.1029/2003RS002916.

Hajj, G. A., L. C. Lee, X. Pi, L. J. Romans, W. S. Schreiner, P. R. Straus, and C. Wang, 2000: COSMIC GPS ionospheric sensing and space weather. *Terr. Atmos. Oceanic Sci.,* **11,** 235–272.

——, and Coauthors, 2004: CHAMP and SAC-C atmospheric occultation results and intercomparisons. *J. Geophys. Res.,* **109,** D06109, doi:10.1029/2003JD003909.

Healy, S., and J. Eyre, 2000: Retrieving temperature, water vapour and surface pressure information from a refractive-index profiles derived by radio occultation: A simulation study. *Quart. J. Roy. Meteor. Soc.,* **126,** 1661–1683.

——, and J.-N. Thépaut, 2006: Assimilation experiments with CHAMP GPS radio occultation measurements. *Quart. J. Roy. Meteor. Soc.,* **132,** 605–623.

Highwood, E. J., and B. J. Hoskins, 1998: The tropical tropopause. *Quart. J. Roy. Meteor. Soc.,* **124,** 1579–1604.

Ho, S.-P., Y.-H. Kuo, Z. Zeng, and T. Peterson, 2007: A comparison of lower stratosphere temperature from microwave measurements with CHAMP GPS RO data. *Geophys. Res. Lett.,* **34,** L15701, doi:10.1029/2007GL030202.

——, M. Goldberg, Y.-H. Kuo, C. Z. Zou, and W. Schreiner, 2008: The application of COSMIC data for improving stratospheric trend analyses: The preliminary results. *Terr. Atmos. Oceanic Sci.,* in press.

Jensen, A. S., M. S. Lohmann, H.-H. Benzon, and A. S. Nielsen, 2003: Full spectrum inversion of radio occultation signals. *Radio Sci.,* **38,** 1040, doi:10.1029/2002RS002763.

Jensen, E., and L. Pfister, 2004: Transport and freeze-drying in the tropical tropopause layer. *J. Geophys. Res.,* **109,** D02207, doi:10.1029/2003JD004022.

Kalnay, E., and Coauthors, 1996: The NCEP/NCAR reanalysis project. *Bull. Amer. Meteor. Soc.,* **77,** 437–471.

Karl, T. R., S. J. Hassol, C. D. Miller, and W. L. Murray, Eds., 2006: *Temperature trends in the lower atmosphere: Steps for understanding and reconciling differences.* A Report by the Climate Change Science Program and Subcommittee on Global Change Research, 180 pp. [Available online at www.climatescience.gov/Library/sap/sap1-1/finalreport/default.htm.]

Kuo, Y.-H., T.-K. Wee, S. Sokolovskiy, C. Rocken, W. Schreiner, D. Hunt, and R. A. Anthes, 2004: Inversion and error estimation of GPS radio occultation data. *J. Meteor. Soc. Japan,* **82,** 507–531.

Kursinski, E. R., G. A. Hajj, K. R. Hardy, J. T. Schofield, and R. Linfield, 1997: Observing Earth's atmosphere with radio occultation measurements. *J. Geophys. Res.,* **102,** 23 429–23 465.

Lei, J., and Coauthors, 2007: Comparison of COSMIC ionospheric measurements with ground-based observations and model predictions: Preliminary results. *J. Geophys. Res.,* **112,** A07308, doi:10.1029/2006JA012240.

Lindal, G. F., G. E. Wood, H. B. Hotz, D. N. Sweetnam, V. R. Eshleman, and G. L. Tyler, 1983: The atmosphere of Titan: An analysis of the Voyager 1 radio occultation measurements. *Icarus,* **53,** 348–363.

Mannucci, A. J., C. O. Ao, T. P. Yunck, L. E. Young, G. A. Hajj, B. A. Iijima, D. Kuang, T. K. Meehan, and S. S. Leroy, 2006: Generating climate benchmark atmospheric soundings using GPS occultation data. *Atmospheric and Environmental Remote Sensing Data Processing and Utilization II: Perspective on Calibration/Validation Initiatives and Strategies,* A. H. L. Huang and H. J. Bloom, Eds., International Society for Optical Engineering (SPIE Proceedings, Vol. 6301), art. 630108, doi:10.1117/12.683973.

Mears, C. A., M. C. Schabel, and F. J. Wentz, 2003: A reanalysis of the MSU channel 2 tropospheric temperature record. *J. Climate,* **16,** 3650–3664.

Ohring, G., B. Wielicki, R. Spencer, B. Emery, and R. Atlas, 2005: Satellite instrument calibration for measuring global climate change—Report of a workshop. *Bull. Amer. Meteor. Soc.,* **86,** 1303–1313.

Palmer, P., J. Barnett, J. Eyre, and S. Healy, 2000: A non-linear optimal estimation inverse method for radio occultation measurements of temperature, humidity, and surface pressure. *J. Geophys. Res.,* **105,** 17 513–17 526.

Powers, J. G., A. J. Monaghan, A. M. Cayette, D. H. Bromwich, Y.-H. Kuo, and K. W. Manning, 2003: Real-time mesoscale modeling over Antarctica: The Antarctica Mesoscale Prediction System. *Bull. Amer. Meteor. Soc.,* **84,** 1533–1545.

Randel, W. J., and F. Wu, 2005: Kelvin wave variability near the equatorial tropopause observed in GPS radio occultation measurements. *J. Geophys. Res.,* **110,** D03102, doi:10.1029/2004JD005006.

——, ——, and W. Rivera Rios, 2003: Thermal variability of the tropical tropopause region derived from GPS/MET observations. *J. Geophys. Res.,* **108,** 4024, doi:10.1029/2002JD002595.

Rocken, C., and Coauthors, 1997: Analysis and validation of GPS/MET data in the neutral atmosphere. *J. Geophys. Res.,* **102** (D25), 29 849–29 866.

Santer, B. D., and Coauthors, 2003: Contributions of anthropogenic and natural forcing to recent tropopause height changes. *Science,* **301,** 479–483.

Scherliess, L., R. W. Schunk, J. J. Sojka, D. C. Thompson, and L. Zhu, 2006: Utah State University Global Assimilation of Ionospheric Measurements Gauss–Markov Kalman filter model of the ionosphere: Model description and validation. *J. Geophys. Res.,* **111,** A11315, doi:10.1029/2006JA011712.

Schreiner, W. S., S. V. Sokolovskiy, C. Rocken, and D. C. Hunt, 1999: Analysis and validation of GPS/MET radio occultation data in the ionosphere. *Radio Sci.,* **34,** 949–966.

——, C. Rocken, S. Sokolovskiy, S. Syndergaard, and D. Hunt, 2007: Estimates of the precision of GPS radio occultations from the COSMIC/FORMOSAT-3 mission. *Geophys. Res. Lett.,* **34,** L04808, doi:10.1029/2006GL027557.

Schunk, R. W., L. Scherliess, J. J. Sojka, and D. Thompson, 2004: Global Assimilation of Ionospheric Measurements (GAIM). *Radio Sci.,* **39,** RS1S02, doi:10.1029/2002RS002794.

Seidel, D. J., and W. J. Randel, 2006: Variability and trends in the global tropopause estimated from radiosonde data. *J. Geophys. Res.,* **111,** D21101, doi:10.1029/2006JD007363.

Simmons, A., S. Uppala, D. Dee, and S. Kobayashi, 2007: ERA-Interim: New ECMWF reanalysis products from 1989 onwards. ECMWF Newsletter No. 110, 25–35.

Sokolovskiy, S., 2001: Tracking tropospheric radio occultation signals from low Earth orbit. *Radio Sci.,* **36,** 483–498.

——, 2003: Effect of superrefraction on inversions of radio occultation signals in the lower troposphere. *Radio Sci.,* **38,** 1058, doi:10.1029/2002RS002728.

——, C. Rocken, D. Hunt, W. Schreiner, J. Johnson, D. Masters, and S. Esterhuizen, 2006a: GPS profiling of the lower troposphere from space: Inversion and demodulation of the open-loop radio occultation signals. *Geophys. Res. Lett.,* **33,** L14816, doi:10.1029/2006GL026112.

——, Y.-H. Kuo, C. Rocken, W. S. Schreiner, D. Hunt, and R. A. Anthes, 2006b: Monitoring the atmospheric boundary layer by GPS radio occultation signals recorded in the open-loop mode. *Geophys. Res. Lett.,* **33,** L12813, doi:10.1029/2006GL025955.

Syndergaard, S., W. S. Schreiner, C. Rocken, D. C. Hunt, and K. F. Dymond, 2006: Preparing for COSMIC: Inversion and analysis of ionospheric data products. *Atmosphere and Climate: Studies by Occultation Methods,* U. Foelsche, G. Kirchengast, and A. K. Steiner, Eds., Springer, 137–146.

Trenberth, K. E., B. Moore, T. R. Karl, and C. Nobre, 2006: Monitoring and prediction of the Earth's climate: A future perspective. *J. Climate,* **19,** 5001–5008.

Wang, C., G. Hajj, X. Pi, I. G. Rosen, and B. Wilson, 2004: Development of the Global Assimilative Ionospheric Model. *Radio Sci.,* **39,** RS1S06, doi:10.1029/2002RS002854.

Ware, R., and Coauthors, 1996: GPS sounding of the atmosphere from low Earth orbit: Preliminary results. *Bull. Amer. Meteor. Soc.,* **77,** 19–40.

Wickert, J., and Coauthors, 2001: Atmosphere sounding by GPS radio occultation: First results from CHAMP. *Geophys. Res. Lett.,* **28,** 3263–3266.

WMO, 1996: *Guide to Meteorological Instruments and Methods of Observation.* 6th ed. WMO No. 8.

Xie, F., S. Syndergaard, E. R. Kursinski, and B. M. Herman, 2006: An approach for retrieving marine boundary layer refractivity from GPS occultation data in the presence of superrefraction. *J. Atmos. Oceanic Technol.,* **23,** 1629–1644.

Yunck, T. P., C.-H. Liu, and R. Ware, 2000: A history of GPS sounding. *Terr. Atmos. Oceanic Sci.,* **11,** 1–20.